Hindawi
Geofluids
Volume 2019, Article ID 4783514, 18 pages
https://doi.org/10.1155/2019/4783514

Research Article

Degassing and Cycling of Mercury at Nisyros Volcano (Greece)

A. L. Gagliano[1], **S. Calabrese**[1,2], **K. Daskalopoulou**[2,3], **J. Cabassi**[4,5], **F. Capecchiacci**[4,5], **F. Tassi**[4,5], **S. Bellomo**[1], **L. Brusca**[1], **M. Bonsignore**[6], **S. Milazzo**[2], **G. Giudice**[1], **L. Li Vigni**[1], **F. Parello**[2] and **W. D'Alessandro**[1]

[1]*Istituto Nazionale di Geofisica e Vulcanologia, Sezione di Palermo, Via U. La Malfa 153, 90146 Palermo, Italy*
[2]*University of Palermo, Dip. Scienze della Terra e del Mare, Via Archirafi 36, 90123 Palermo, Italy*
[3]*National and Kapodistrian University of Athens, Dept. of Geology and Geoenvironment, Panestimioupolis, 15784, Ano Ilissia, Greece*
[4]*University of Florence, Dip. Scienze della Terra, Via La Pira 4, 50121 Florence, Italy*
[5]*Consiglio Nazionale delle Ricerche, IGG, Via La Pira 4, 50121 Florence, Italy*
[6]*Consiglio Nazionale delle Ricerche, IAMC, UOS di Capo Granitola, via del Mare 3, 91021 Campobello di Mazara (TP), Italy*

Correspondence should be addressed to S. Calabrese; sergio.calabrese@gmail.com

Received 7 February 2019; Revised 6 May 2019; Accepted 1 July 2019; Published 14 August 2019

Guest Editor: Guodong Zheng

Copyright © 2019 A. L. Gagliano et al. This is an open access article distributed under the Creative Commons Attribution License, which permits unrestricted use, distribution, and reproduction in any medium, provided the original work is properly cited.

Nisyros Island (Greece) is an active volcano hosting a high-enthalpy geothermal system. During June 2013, an extensive survey on Hg concentrations in different matrices (fumarolic fluids, atmosphere, soils, and plants) was carried out at the Lakki Plain, an intracaldera area affected by widespread soil and fumarolic degassing. Concentrations of gaseous elemental mercury (GEM), together with H_2S and CO_2, were simultaneously measured in both the fumarolic emissions and the atmosphere around them. At the same time, 130 samples of top soils and 31 samples of plants (*Cistus creticus* and *salvifolius* and *Erica arborea* and *manipuliflora*) were collected for Hg analysis. Mercury concentrations in fumarolic gases ranged from 10,500 to 46,300 ng/m^3, while Hg concentrations in the air ranged from high background values in the Lakki Plain caldera (10-36 ng/m^3) up to 7100 ng/m^3 in the fumarolic areas. Outside the caldera, the concentrations were relatively low (2-5 ng/m^3). The positive correlation with both CO_2 and H_2S in air highlighted the importance of hydrothermal gases as carrier for GEM. On the other hand, soil Hg concentrations (0.023-13.7 μg/g) showed no significant correlations with CO_2 and H_2S in the soil gases, whereas it showed a positive correlation with total S content and an inverse one with the soil pH, evidencing the complexity of the processes involving Hg carried by hydrothermal gases while passing through the soil. Total Hg concentrations in plant leaves (0.010-0.112 μg/g) had no direct correlation with soil Hg, with *Cistus* leaves containing higher values of Hg with respect to *Erica*. Even though GEM concentrations in the air within the caldera are sometimes orders of magnitude above the global background, they should not be considered dangerous to human health. Values exceeding the WHO guideline value of 1000 ng/m^3 are very rare (<0.1%) and only found very close to the main fumarolic vents, where the access to tourists is prohibited.

1. Introduction

Volcanoes and geothermal areas are natural sources of environment pollutants potentially dangerous for human health. Paroxysmal eruptions and passive degassing emit huge amounts of gases such as CO_2, H_2S, SO_2, and HF, including gaseous elemental mercury (GEM) [1–4]. Trace metals, being associated with uprising gases, are usually found at considerable concentrations in hydrothermal fluids [5]. Even at very low concentrations, they can have a strong impact on the atmosphere and hydrosphere and consequently on the biosphere [6].

Among the volcanic trace volatile elements, mercury (Hg) is one of the most environmentally significant [7] because of its extreme mobility and toxicity [8]. The biogeochemistry of Hg is extremely complex due to the exchanges

between atmospheric, terrestrial, and marine pools [9]. These processes are mainly driven by microbial activity, dark abiotic and photochemical reactions affecting Hg speciation and bioaccumulation [10]. It is emitted in several forms: elemental (metallic) Hg and inorganic and organic Hg compounds. Metallic Hg (Hg^0) is highly volatile due to its high vapour pressure and may experience long-range transport in the air due to its relatively long half-life in the atmosphere (1-2 years [11]). Monovalent and divalent Hg are both soluble in water; divalent Hg (Hg^{II}) is more stable and common in the environment than monovalent (Hg^I). This form also may undergo complexation, precipitation with inorganic ligands, and sorption onto the soil matrix. The toxicological properties of Hg for the environment and human health depend on the physical and chemical form in which it occurs. Hg vapours, for example, are very dangerous if inhaled, due to their ability to reach the lungs causing pulmonary oedema, pain, and peeling of the respiratory epithelium of the bronchi [12, 13].

Mercury, as a constituent of volcanic and geothermal fluids [14, 15], is discharged in water and released into the atmosphere as Hg^0 being associated with reducing noncondensable gases [16, 17].

In the last decades, many authors underlined the correlation between Hg and H_2S in discharged hydrothermal fluids (e.g., [18]), as testified by the formation of solid cinnabar (HgS) at the fumarolic vents. Hydrogen sulphide is a toxic pollutant; it is corrosive and poses severe concerns for human health [19, 20].

Nisyros Island is a quiescent volcano releasing hydrothermal gases from several fumarolic emissions and also diffusively through the soil. The hydrothermal fluids of Nisyros are rich in H_2S [21–23], and their diffuse emission creates an extremely acidic environment in soils affected by the hydrothermal degassing [24, 25].

Here, we report the results of an extensive survey on Hg concentrations in different media (fumarolic fluids, atmosphere, soils, and plants) at the Lakki Plain, an area intensively impacted by hydrothermal degassing on Nisyros Island. Even though the geogenic degassing of Nisyros Island has been greatly studied, most of the research conducted was mainly concentrated on the gaseous C compounds and the noble gas composition of the fumaroles. The significance and novelty of this work, with respect to the existing literature, is to add Hg on the puzzle. Furthermore, to the best of our knowledge, this is so far the first study that attempts to define the Hg cycling in an active volcanic/geothermal system by taking into consideration such a great variety of media. Gaseous elemental mercury (GEM) concentrations, together with H_2S and CO_2 in soil gas, were determined in both the fumarolic emissions and ambient air. Similarly, the relationships between fumarolic activity and Hg in the soils were investigated, comparing Hg concentrations to temperature, pH, hydrothermal gas, and the elemental concentrations of C, N, and S measured in the same soils. Leaves of two plant species (*Cistus* and *Erica*) were also collected and their Hg and S contents determined. Finally, a preliminary estimation of the Hg output to the atmosphere from the hydrothermal area of Nisyros was carried out.

2. Study Area

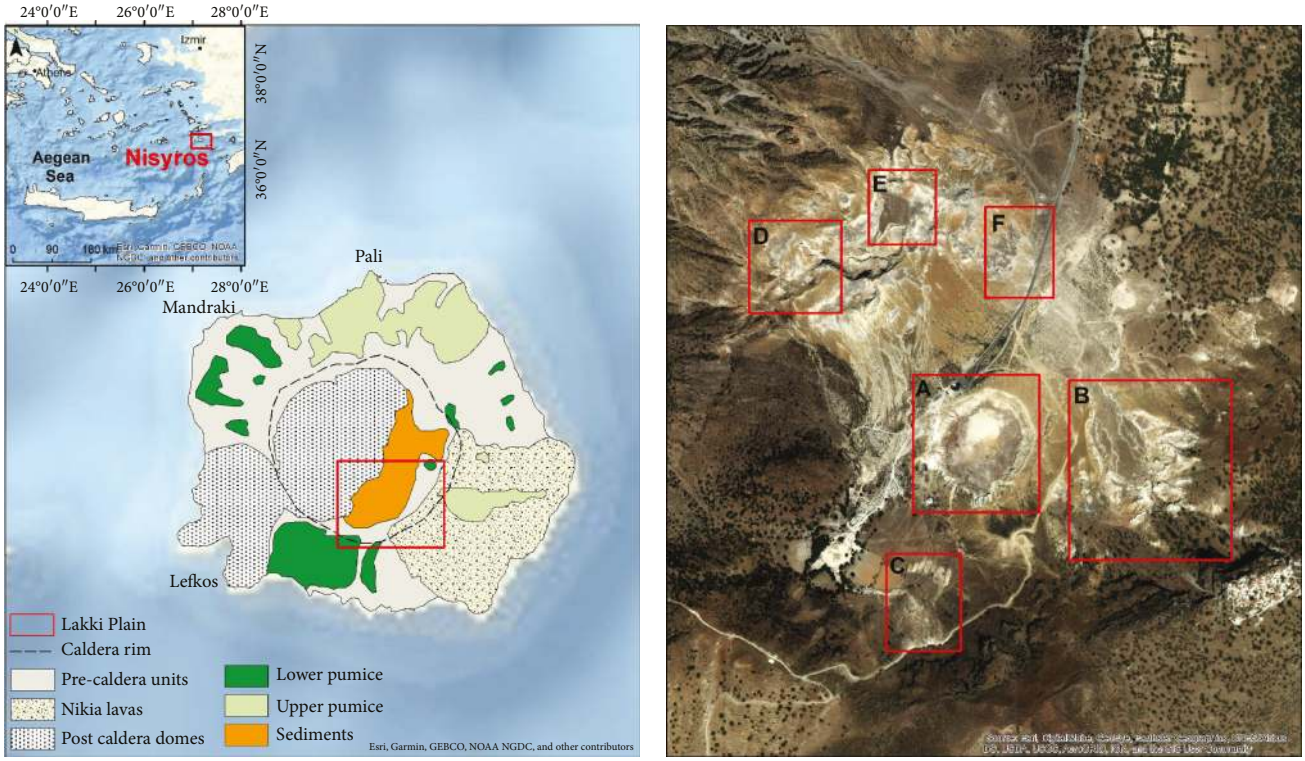
Nisyros Island (Figure 1) is a quiescent volcano located in the easternmost volcanic group of the South Aegean Active Volcanic Arc (SAAVA [26]). The volcanic edifice developed in the last 200 ka through five distinguished stages [27, 28] led to the formation of a caldera of about 4 km in diameter. The most recent activity consisted of hydrothermal explosions forming several phreatic craters, the last of which occurred in 1887 [27]. The Lakki Plain (Figure 1) represents the southeastern remnants of the calderic depression after the emplacement of a series of volcanic domes filling up the northwestern part. Fumarolic fields are currently active in this area, mainly within the hydrothermal craters strongly controlled by fracturing along the main NW- and NE-trending active fault systems [29], and are fed by a >1000 m deep hydrothermal system having a temperature of 300-350°C [30, 31]. The hydrothermal craters form three main groups (Figure 1): the oldest comprises the Kaminakia craters, the second consists of the Stefanos crater, whereas the third corresponds to the youngest area where a postcalderic dome (Lofos) is placed and includes the Phlegeton, Megalos Polybotes, and Mikros Polybotes craters [31, 32]. Water vapour (91-99%) is the main component of the fumarolic fluids, followed by CO_2 and H_2S [22]. The estimated total CO_2 and H_2S outputs are close to 1 kg/s and <0.3 kg/s, respectively [31, 32].

3. Materials and Methods

After the collection of few samples in 2009 and 2010, a multidisciplinary field campaign was carried out on June 2013 at the Lakki Plain, where soil gases, soils, and vegetation were sampled, and Hg, H_2S, and CO_2 concentrations in the air were measured.

A total of 106 soil gas samples was collected at the Lakki Plain mostly in the fumarolic areas of Kaminakia, Stefanos, Mikros Polybotes, and Phlegeton craters and in the areas of Ramos and Lofos (Figure 1). Soil gases were sampled at 50 cm depth using a Teflon tube of 5 mm ID equipped with a tight plastic syringe to avoid air contamination. Soil gas sampling sites were the same as those of the top soils. H_2S and CO_2 analysis was carried out on the overpressurised vials using a Micro GC MSHA CP-4900 having 3 independent modules. Soil temperature was measured at 20 cm depth by using thermal probes and a digital thermometer; these measurements were carried out 10–15 min after the insertion of the thermal probe in the soil in order to achieve thermal equilibrium.

Top soils were collected from the first 3 cm depth at 130 spots at the Lakki Plain. Soil samples were dried, homogenized, and powdered. An aliquot of the homogenized samples was used for the analysis of total Hg, which was performed using a DMA-80 analyser (an atomic absorption spectrophotometer, Milestone, Wesleyan University, Middletown, CT, USA). About 10 mg of dry soil was loaded into specific nickel boats and analysed according to the US-EPA 7473 method [33]. Accuracy was checked by running replicates of the reference materials NCSDC7701



(a) (b)

Figure 1: Simplified geologic map of the island of Nisyros (a) and sampling areas within the Lakki Plain (b). A = Stefanos crater; B = Kaminakia crater; C = Ramos fumaroles; D = Phlegeton crater; E = Mikros Polybotes; F = Lofos dome.

(0.015 ± 0.006 mg/kg) and MESS3 (0.091 ± 0.009 mg/kg). Bench quality control material was measured at the start of each analytical run (set of 15 samples) for quality assurance and control. The measured values were, on average, within ±8% of the recommended values.

Total C, N, and S were analysed on powdered samples by elemental analysis (Elementar Vario EL Cube, Hanau). The technique is based on "purge and trap" separation (C, N, and S), following high-temperature incineration (induction furnace) in a pure oxygen atmosphere and at a constant temperature exceeding 1150°C for the sample, with WO_3 as catalyst. Helium was used as the carrier gas. Detection limits were 0.04 wt% for C and 0.003 wt% for N and S.

Soil pH values were measured using a specific combination electrode on soil suspensions that were made with deionized water with a soil/solution weight ratio of 1/2.5 [34].

A passive biomonitoring survey was carried out in order to determine the total Hg content in two local spontaneous plants and evaluate the possible contamination by Hg gas emissions. The collected vegetation consisted of 17 leaf samples of the genus *Erica* (*manipuliflora* and *arborea* spp.) and 14 leaf samples of the genus *Cistus* (*creticus* and *salvifolius* spp.). Both the plant species have evergreen leaves and grow widespread as small shrubs (10-50 cm height) in the Lakki Plain where soil degassing is at a lower level. To enhance the interpretation, soil samples were collected along a buffer area of few tens of centimetres close to the sampled plants. One sample of vegetation and soil was collected outside the caldera as local background blank. The sampling sites and the sampled plants were chosen randomly; for each site, three separate plants in a buffer area of 1.5 m were sampled and merged to obtain the final sample. Vegetation samples were dried in the oven at temperature below 40°C and powdered by agate planetary ball mill to avoid contamination. Analysis of total Hg was made with the use of PerkinElmer Inc. SMS 100 Solid Mercury Analysis. Each sample was heated in an oxygen-rich furnace to release all the decomposition products including Hg. These products were then carried in a stream of O_2 to a catalytic section of the furnace; halogens and/or oxides of N and S were trapped on the catalyst. The remaining vapour was then carried to an amalgamation cell that selectively trapped Hg. After the system was flushed with O_2 to remove any remaining gas or decomposition products, the amalgamation cell was rapidly heated, releasing Hg vapour. Flowing O_2 carried the Hg vapour through an absorbance cell positioned in the light path of a single wavelength atomic absorption spectrophotometer. Absorbance was measured at the 253.7 nm wavelength as a function of the Hg concentration in the sample.

Collection of total gaseous mercury (TGM) was performed with gold-coated bead traps (Au traps), through which atmospheric air was pumped at flow rates between 0.5 and 0.6 L/min [35] over collection periods ranging from 2 to 60 min. At three fumaroles, the gas was collected downstream of a vapour condenser sucking with a

graduated 100 mL syringe and sent to the same Au traps through a three-way valve [36]. The collected Hg was then measured by cold vapour atomic fluorescence spectrometry (CVAFS), based on the conventional thermal-desorption amalgamation technique (relative standard deviation < 15%; EPA Method IO-5; [33, 35, 37]). The results obtained were multiplied by the sampling volume and expressed in ng/m^3.

The simultaneous real-time measurements of gaseous elemental mercury (GEM), CO_2, H_2S, and meteorological parameters (air temperature, pressure, and relative humidity) were carried out by coupling portable instruments (similarly to what was proposed by [20]). GEM was measured with a Lumex® RA-915M, which is an atomic absorption spectrometer with a Zeeman effect with high-frequency modulation of light polarization (ZAAS-HFMLP). The separation of the spectral lines (at $\lambda = 254$ nm) is operated by a permanent external magnetic field, into which a source of radiation (Hg lamp) is placed [38, 39]. The Zeeman background correction and the multipath analytical cell provide high selectivity and sensitivity [39]. The instrument operates at a flow rate of 10 L/min, whereas its rechargeable battery allows up to 8 h of continuous measurements. The detection limit is 2 ng/m^3, while the accuracy of the method is 20% from 2 to 50,000 ng/m^3 [38, 39]. The remaining parameters were measured with a Multi-GAS analyser manufactured by INGV-Palermo. Atmospheric gas was drawn into the sampler with an air pump at 1.2 L/min through a 1 μm Teflon membrane particle filter and was pumped through a CO_2/H_2O gas detector (Licor LI-840 NDIR closed-path spectrometer) and a series of electrochemical sensors for SO_2 (0–200 ppm; 3ST/F electrochemical sensor by City Technology Ltd.) and H_2S (0–50 pm; EZ3H electrochemical sensor by City Technology Ltd.) detection. The sensors were housed in a weather-proof box mounted on a backpack frame and were calibrated, before and after fieldwork, with standard calibration gases (200 ppm SO_2, 50 ppm H_2S, and 3014 ppm CO_2) mixed with ultrapure nitrogen to provide a range of desired concentrations [4, 40].

The spatial coordinates for each concentration value were simultaneously acquired through a GPS signal. All instruments were synchronized and set to high-frequency acquisition (every two seconds: 0.5 Hz). Measurements were carried out along four (Polybotes, Kaminakia, Stefanos, and Lofos) transect walks (about 15 km path, with a mean speed of 1.5 km/h) across the Lakki Plain caldera. The raw data have been processed by a dedicated software (RatioCalc [41]) that allows a derivation of mass ratios of various compounds (e.g., CO_2/H_2S, GEM/CO_2, and GEM/H_2S).

Dataset from the gas soil and air surveys were used to define the threshold values of Hg, H_2S, and CO_2. Data were processed following Sinclair's portioning method extracting the main populations [42]. This method consists in the definition of single populations through the inflection points (main populations) or changes in direction (secondary populations) of the curvature on the probability plot by visual analysis. Finally, data were plotted by using the GIS platform; distribution maps were drawn and ranked according to the identified populations.

4. Results

4.1. Fumarolic Gases and Atmosphere. In 2009, TGM was measured with Au traps in the atmosphere at 9 sampling sites at different distances from the main fumarolic vents. These sampling sites were previously investigated by D'Alessandro et al. [43] measuring H_2S concentrations in the atmosphere with passive samplers. The traps were placed in a range of distance always longer than 10 m and up to about 2 km from the fumarolic vent. Mercury values ranged from 9.4 to 420 ng/m^3 (Table 1). Although not directly comparable due to the different and sometimes not overlapping measuring time intervals (2-60 min for TGM and 4 hours to 5 days for H_2S), the two datasets show a positive correlation (Figure 2), with the highest values close to the fumaroles and the lowest on the caldera rim.

In 2010, further 5 measurements with Au traps were performed. Two measurements were made in the atmosphere at less than 1 m far from the two main fumarolic vents and gave concentrations of 2360 and 4530 ng/m^3 (Table 1). Three fumarolic vents were investigated by performing measurements on the undiluted hydrothermal fluid collected at the outlet of a condenser; results provided values from 10,500 to 46,300 ng/m^3 (Table 1). The composition of the contemporaneously collected gases was published by [44].

In 2013, GEM measured with Lumex® gave atmospheric concentrations from 2 to 7132 ng/m^3. Values measured with the Multi-GAS ranged from 393 μmol/mol, which is the background atmospheric value, up to saturation of the sensor (~4000 μmol/mol) for CO_2, from 0.2 μmol/mol up to saturation of the sensor (~60 μmol/mol) for H_2S, and from 0.39 to 1.34 μmol/mol for SO_2. Saturated values, about 0.1% for CO_2 and 1.6% for H_2S, were not considered for Hg/CO_2 and Hg/H_2S calculations.

4.2. Soils. All parameters measured in the soil samples of the fumarolic areas of the Lakki Plain are shown in Table 2. Total Hg ranged from 0.023 to 13.7 μg/g of dry soil. Soil temperatures measured at 20 cm depth varied between 25.5 and 100°C, while concentrations of H_2S and CO_2 at 50 cm depth ranged from <0.001 to 17.8% vol and from 0.28 to 75.3% vol, respectively. Elemental C, N, and S contents in the soil were in the range 0.06-2.63, 0.004-0.23, and 0.014-56.3 weight %, respectively. Soil pH varied from 0.71 to 7.30.

4.3. Plants. Total Hg concentrations in the leaves collected from the Lakki Plain are summarized in Table 3. Data analysis showed the Hg range from 0.014 to 0.066 μg/g for *Erica* leaves and from 0.010 to 0.112 μg/g for *Cistus* leaves. The Hg concentrations in the soils sampled near the plants vary from 0.045 to 0.619 μg/g with a pH ranging from 4.21 to 5.55 (Table 2). The highest pH value is 7.30 and was measured outside the caldera; the value is representative of the local background for the soils collected close to the plants (Table 2).

5. Discussion

5.1. Mercury in the Fumarolic Fluids of Nisyros. Analyses of Hg directly on fumarolic fluids have rarely been performed.

Table 1: Total gaseous mercury (TGM) measured with Au traps in the atmosphere and in hydrothermal fluids at Nisyros.

Sample		Date (dd/mm/yyyy)	Time (min)	Flux (dm^3/min)	Volume (m^3)	TGM (ng/m^3)
Stefanos 1	(4)	31/08/2009	5	0.5	0.0025	266
Stefanos 2	(5)	31/08/2009	5	0.5	0.0025	163
Emporio	(24)	01/09/2009	50	0.5	0.025	17.3
Volcano Cafe	(8)	01/09/2009	30	0.5	0.015	54.1
Polybotes bottom	(2)	02/09/2009	2	0.5	0.0010	222
Polybotes rim	(3)	02/09/2009	5	0.5	0.0025	133
Kaminakia	(9)	03/09/2009	5	0.5	0.0025	420
Phlegeton	(1)	04/09/2009	5	0.5	0.0025	188
Nikia	(19)	06/09/2009	60	0.6	0.036	9.4
Phlegeton		31/08/2010	5	0.5	0.0025	4530
Kaminakia		31/08/2010	5	0.5	0.0025	2360
AM fumarole		31/08/2010	n.a.	n.a.	0.00025	46,300
K6 fumarole		31/08/2010	n.a.	n.a.	0.0002	41,200
PP9S fumarole		31/08/2010	n.a.	n.a.	0.0002	10,500

Sampling sites of 2009 and IDs in brackets are the same as in [43]; fumaroles sampled in 2010 are the same as in [44]. n.a. = not applicable.

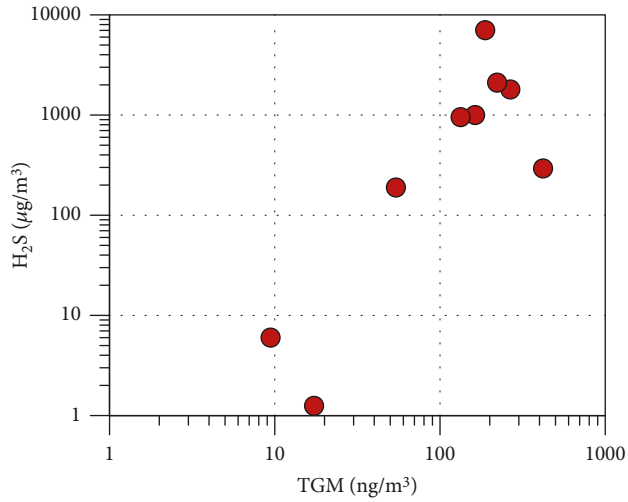


Figure 2: Total gaseous mercury in the atmosphere vs. atmospheric H_2S concentrations. H_2S data from [43].

The values reported in literature related to several fumaroles worldwide [3, 35, 45–49] cover a broad range from 1400 to 1,828,000 ng/m^3 (Table 4). The values resulting from the three fumaroles sampled at Nisyros fall within this range. Correlating the obtained Hg values with the major composition of the fumarolic gases [44], Hg/H_2S and Hg/CO_2 ratios ranging from 0.36×10^{-7} to 3.3×10^{-7} and from 0.76×10^{-8} to 3.5×10^{-8}, respectively, were observed. The results obtained are coherent with values provided by other fumarolic fields at world scale (Table 4).

The measured Hg/H_2S and Hg/CO_2 ratios should be regarded as lower limit values since water soluble Hg^{II} species plausibly are lost within the fumarolic condensate collected by the sampling device. As evidenced in previous studies, the lost Hg fraction could represent a significant part of the total emitted Hg. Bagnato et al. [49] suggested that up to 70% of the total Hg emitted from the Bocca Grande (BG) fumarole (Phlegrean Fields, southern Italy) remained in the collected condensate. However, of the 70 fumarolic samples in which Nakagawa [36, 45, 46] measured Hg both in the gas and in the condensed vapour, only in 8 of the samples was the Hg found in the condensed fraction that represented more than 20% of the total. Nevertheless, further studies will be necessary to ascertain the quantity of Hg lost in the condensed steam in the fumaroles of Nisyros.

5.2. Mercury in the Atmosphere of the Lakki Plain Area. Background values of atmospheric GEM in pristine unpolluted areas in the northern hemisphere are below 2 ng/m^3, though a decreasing trend in the last decades was recognized [50]. In volcanic/geothermal areas, measured values are often significantly higher than the natural background (tens to hundreds of ng/m^3, Table 5). This holds true also for the fumarolic area of the Lakki Plain at Nisyros both for the point measurements with Au traps and for measurements performed along transects with Lumex®.

The data acquired in the air with the Lumex® and MultiGAS were plotted as described by Sinclair [42] and are shown in Figure 3. The CO_2 probability plot (Figure 3(a)) identifies three main populations (A, B, and C). The A population comprises 64.6% of the data with values ranging from 392 to 431 ppm and refers to the local atmospheric CO_2 background, which is close to the global atmospheric value of unpolluted air in 2013 (395 ppm [51]). Population B (33.3% of the data; CO_2 431-561 ppm) is the population with CO_2 level slightly higher than average atmospheric air, probably due to diffuse soil degassing. Population C (2.1% of the data) includes the highest values (up to >4000 ppm), indicating a significant fumarolic CO_2 contribution to the atmosphere.

Based on the probability plot (Figure 3(b)), the H_2S dataset can be divided into four populations: A includes very low H_2S concentrations (<0.47 ppm, 5% of the values); B population with values from 0.47 to 2.11 ppm (50% of the data) indicating a slight fumarolic contribution; C

Table 2: Analytical composition of soils and soil gases at the Lakki caldera.

Site	E	N	Hg (μg/g)	N (%)	C (%)	S (%)	pH	H_2S (%)	CH_4 (%)	CO_2 (%)	T (°C @ 20 cm)
1*	518465	4049840	0.023	n.d.	n.d.	0.014	7.30	n.d.	n.d.	n.d.	n.m.
Mandraki	512418	4051816	0.039	n.d.	n.d.	n.d.	n.m.	n.d.	n.d.	n.d.	n.m.
2*	515026	4047948	0.18	n.d.	n.d.	1.319	4.60	n.d.	n.d.	n.d.	n.m.
3*	515008	4047754	0.40	n.d.	n.d.	0.728	5.20	n.d.	n.d.	n.d.	n.m.
4*	514836	4047603	0.58	n.d.	n.d.	0.723	4.74	n.d.	n.d.	n.d.	n.m.
5*	514702	4047912	0.40	n.d.	n.d.	0.524	4.70	n.d.	n.d.	n.d.	n.m.
6*	514617	4048285	0.40	n.d.	n.d.	0.392	5.55	n.d.	n.d.	n.d.	n.m.
7*	514608	4048481	0.37	n.d.	n.d.	0.306	4.95	n.d.	n.d.	n.d.	n.m.
8*	514541	4048566	0.49	n.d.	n.d.	0.786	4.86	n.d.	n.d.	n.d.	n.m.
9*	514659	4048676	0.54	n.d.	n.d.	0.451	4.21	n.d.	n.d.	n.d.	n.m.
10*	514830	4048652	0.14	n.d.	n.d.	1.049	4.80	n.d.	n.d.	n.d.	n.m.
11*	514861	4048610	0.21	n.d.	n.d.	1.115	5.02	n.d.	n.d.	n.d.	n.m.
12*	514979	4048382	0.18	n.d.	n.d.	0.575	5.16	n.d.	n.d.	n.d.	n.m.
13*	515081	4048259	0.15	n.d.	n.d.	1.155	4.92	n.d.	n.d.	n.d.	n.m.
14*	515130	4048399	0.25	n.d.	n.d.	0.741	5.31	n.d.	n.d.	n.d.	n.m.
15*	515210	4048719	0.21	n.d.	n.d.	0.764	5.48	n.d.	n.d.	n.d.	n.m.
16*	515402	4048152	0.36	n.d.	n.d.	0.666	4.87	n.d.	n.d.	n.d.	n.m.
17*	515296	4048377	0.64	n.d.	n.d.	0.426	5.04	n.d.	n.d.	n.d.	n.m.
N-St-1	514990	4048141	0.28	n.d.	n.d.	9.215	2.42	n.d.	n.d.	n.d.	n.m.
N-St-3	515020	4048123	0.39	n.d.	n.d.	1.643	2.66	n.d.	n.d.	n.d.	n.m.
N-St-5	515050	4048108	1.57	n.d.	n.d.	7.278	2.70	n.d.	n.d.	n.d.	n.m.
N-St-7	515096	4048083	1.28	n.d.	n.d.	8.566	2.58	n.d.	n.d.	n.d.	n.m.
N-St-9	515156	4048052	0.42	n.d.	n.d.	6.960	2.07	n.d.	n.d.	n.d.	n.m.
N-St-10	515131	4048186	0.29	n.d.	n.d.	3.988	2.31	n.d.	n.d.	n.d.	n.m.
N-St-11	515119	4048163	0.25	n.d.	n.d.	2.415	2.97	n.d.	n.d.	n.d.	n.m.
N-St-13	515092	4048121	1.25	n.d.	n.d.	4.263	3.04	n.d.	n.d.	n.d.	n.m.
N-St-15	515048	4048049	1.77	n.d.	n.d.	6.231	2.71	n.d.	n.d.	n.d.	n.m.
N-St-17	515032	4048046	1.25	n.d.	n.d.	9.823	2.65	n.d.	n.d.	n.d.	n.m.
N-St-19	515015	4047998	0.81	n.d.	n.d.	17.844	1.92	n.d.	n.d.	n.d.	n.m.
N-St-21	514998	4047968	0.31	n.d.	n.d.	7.576	2.63	n.d.	n.d.	n.d.	n.m.
N-St-23	515115	4048009	0.39	n.d.	n.d.	11.536	2.00	n.d.	n.d.	n.d.	n.m.
N-St-24	515160	4048086	0.61	n.d.	n.d.	10.849	2.13	n.d.	n.d.	n.d.	n.m.
N-St-27	515021	4048167	0.20	n.d.	n.d.	6.597	2.12	n.d.	n.d.	n.d.	n.m.
N-St-28	514958	4048098	0.31	n.d.	n.d.	4.751	2.05	n.d.	n.d.	n.d.	n.m.
023 A	514689	4048508	1.59	0.053	0.800	8.447	1.87	10.28	0.092	47.35	n.m.
024 A	514677	4048516	0.72	0.024	0.261	0.869	2.79	17.75	0.15	75.27	n.m.
025 A	514663	4048529	1.78	0.021	0.421	2.569	1.96	14.93	0.13	64.31	n.m.
026 A	514652	4048510	0.15	0.018	0.060	0.779	2.98	7.63	0.083	45.21	n.m.
027 A	514667	4048507	0.23	0.027	0.103	1.632	2.92	10.20	0.11	53.84	n.m.
028 A	514695	4048526	0.21	0.035	0.097	8.916	1.14	6.82	0.067	35.73	n.m.
029 A	514706	4048510	0.71	0.011	0.070	3.492	2.77	n.d.	n.d.	n.d.	n.m.
030 A	514661	4048504	0.34	0.013	0.328	1.245	2.60	17.83	0.15	75.22	n.m.
031 A	514644	4048505	1.48	0.009	0.074	6.968	2.02	7.01	0.073	38.55	n.m.
032 A	514635	4048488	0.33	0.013	0.095	1.986	2.99	5.67	0.071	36.07	n.m.
033 A	514643	4048490	3.44	0.007	0.198	16.260	1.30	10.06	0.10	56.13	n.m.
034 A	514621	4048490	0.41	0.019	0.070	2.536	2.96	n.d.	n.d.	n.d.	n.m.
035 A	515124	4048615	0.81	0.020	0.443	24.468	1.05	n.d.	n.d.	n.d.	n.m.

Table 2: Continued.

Site	E	N	Hg (μg/g)	N (%)	C (%)	S (%)	pH	H_2S (%)	CH_4 (%)	CO_2 (%)	T (°C @ 20 cm)
036 A	515148	4048631	0.46	0.065	0.424	1.057	2.58	bdl	0.04	9.26	n.m.
037 A	515157	4048651	1.09	0.009	0.159	0.915	2.73	0.005	0.011	5.80	n.m.
039 A	515475	4048182	0.34	0.022	0.367	0.783	4.15	bdl	0.0002	2.27	n.m.
040 A	515500	4048166	0.68	0.040	0.693	1.045	3.15	bdl	0.0004	8.99	n.m.
041 A	515510	4048159	5.03	0.016	0.418	2.593	1.39	0.66	0.48	26.32	n.m.
042 A	515535	4048127	0.76	0.032	0.388	33.506	1.92	0.19	0.24	13.25	n.m.
043 A	515553	4048105	0.54	0.021	0.228	1.973	3.35	0.012	0.0019	13.50	n.m.
044 A	515554	4048112	0.33	0.079	0.974	2.424	3.73	bdl	0.0005	1.60	n.m.
045 A	515394	4048180	0.62	0.019	0.434	4.352	2.79	0.013	0.14	13.10	n.m.
047 A	515465	4048096	0.19	0.035	0.587	0.254	4.80	bdl	0.0005	7.66	n.m.
048 A	515409	4048079	0.11	0.010	0.255	1.322	2.88	0.016	0.11	8.36	n.m.
049 A	515414	4048050	0.79	0.020	0.961	2.672	1.87	bdl	0.49	30.67	n.m.
050 A	515418	4048013	0.61	0.022	0.935	2.159	1.64	2.15	0.90	43.68	n.m.
051 A	515432	4048003	0.32	0.011	0.151	1.512	3.32	bdl	0.22	27.23	n.m.
053 A	515482	4047984	1.05	0.016	0.259	3.954	3.28	0.022	0.25	25.17	n.m.
054 A	515512	4047995	0.15	0.021	0.220	0.933	3.27	n.d.	n.d.	n.d.	n.m.
186 A	515546	4048080	1.22	0.023	0.243	4.280	3.45	0.10	0.30	25.24	n.m.
189 A	515530	4047998	0.14	0.027	0.173	1.238	3.41	bdl	0.0015	5.25	n.m.
212 A	515204	4048707	0.37	0.093	1.777	1.018	3.77	bdl	0.0003	3.36	n.m.
239 A	514958	4048062	0.20	0.009	0.164	40.328	1.33	0.19	0.023	2.80	n.m.
240 A	514990	4048077	0.31	0.006	0.107	4.842	2.48	n.d.	n.d.	n.d.	n.m.
241 A	515032	4048070	0.81	0.022	0.382	5.690	1.25	17.12	0.68	72.01	n.m.
242 A	515024	4048127	0.23	0.021	0.081	1.653	3.47	0.10	0.028	7.30	n.m.
244 A	515088	4048170	0.39	0.024	0.194	1.497	3.17	0.015	0.052	13.83	n.m.
247 A	515100	4048146	0.34	0.034	0.451	1.752	2.80	0.006	0.0008	9.53	n.m.
248 A	515122	4048111	0.41	0.014	0.178	3.216	2.23	1.67	0.16	20.21	n.m.
249 A	515107	4048092	0.21	0.032	0.782	5.172	2.00	n.d.	n.d.	n.d.	n.m.
251 A	515081	4048103	1.44	0.059	0.637	4.563	2.73	bdl	0.0005	9.50	n.m.
254 A	515013	4048047	0.82	0.046	1.047	3.610	1.59	13.75	0.58	61.71	n.m.
255 A	515039	4048033	0.63	0.051	0.780	56.276	2.22	14.97	0.70	68.74	n.m.
256 A	515020	4047981	0.58	0.013	0.252	2.399	1.55	0.087	0.052	6.46	n.m.
257 A	514986	4047992	0.58	0.024	0.728	2.908	1.68	1.79	0.26	29.13	n.m.
259 A	515143	4048093	0.48	0.009	0.152	10.040	1.77	6.86	0.22	32.79	n.m.
N301	515310	4048583	0.30	0.058	0.868	0.727	4.35	bdl	0.0002	0.40	27.3
N302	515384	4048514	0.33	0.031	0.596	0.695	4.09	bdl	0.0005	0.86	30.5
N303	515479	4048463	0.70	0.230	2.625	1.521	3.75	0.048	0.0004	1.55	30.5
N304	514864	4048679	0.47	0.006	0.073	1.956	1.66	9.97	0.21	62.78	66.2
N305	514856	4048673	0.33	0.007	0.091	3.981	1.45	12.63	0.21	63.93	100.0
N307	514848	4048677	0.47	0.010	0.118	3.730	1.28	16.84	0.26	74.73	53.5
N308	514851	4048680	0.27	0.009	0.088	3.461	1.22	16.47	0.25	74.90	61.1
N309	515695	4048364	0.41	0.031	0.419	8.140	3.39	0.008	0.077	21.24	32.2
N310	515688	4048334	0.50	0.149	1.875	1.215	3.56	0.11	0.0018	20.25	31.1
N311	515663	4048292	0.15	0.200	2.337	1.172	3.61	0.002	0.0015	8.10	30.9
N312	515658	4048288	0.13	0.030	0.427	2.740	3.15	bdl	0.006	26.14	34.9
N313	515227	4048688	0.17	0.046	0.612	0.407	4.20	bdl	0.0005	0.99	36.7
N314	515207	4048667	0.64	0.022	0.300	2.017	2.65	bdl	Bdl	2.07	33.6
N315	515190	4048650	0.26	0.104	2.265	0.772	3.66	bdl	0.0006	6.09	38.9
N316	515173	4048628	0.21	0.058	1.144	0.953	3.52	bdl	0.001	10.21	44.4
N317	515153	4048604	0.22	0.020	0.563	16.470	1.15	0.025	0.06	12.64	54.0

Table 2: Continued.

Site	E	N	Hg (μg/g)	N (%)	C (%)	S (%)	pH	H_2S (%)	CH_4 (%)	CO_2 (%)	T (°C @ 20 cm)
N318	515134	4048595	0.32	0.028	0.743	5.035	1.50	0.68	0.10	15.61	51.5
N319	515109	4048583	0.17	0.016	0.171	3.427	1.32	0.004	0.044	10.57	45.9
N320	515095	4048585	0.47	0.029	0.801	3.667	1.49	1.15	0.13	20.46	59.4
N321	515092	4048601	0.70	0.007	0.069	1.620	2.34	0.006	0.03	6.39	43.0
N323	515126	4048638	2.15	0.004	0.109	11.050	1.15	11.38	0.46	59.42	69.8
N324	515139	4048658	0.28	n.d.	n.d.	n.d.	0.78	bdl	0.67	75.00	53.0
N325	515162	4048676	0.23	0.006	0.125	2.415	1.18	0.19	0.09	13.18	48.0
N326	515174	4048697	1.12	0.008	0.245	2.506	1.34	1.61	0.17	21.95	56.4
N327	515621	4048254	0.15	0.016	0.373	3.286	1.48	8.75	1.26	69.20	59.5
N328	515640	4048269	0.29	0.049	0.358	0.900	2.74	bdl	0.16	15.86	28.3
N329	515590	4048259	0.22	0.127	1.928	1.711	3.60	bdl	0.0005	0.38	30.2
N330	515573	4048248	0.44	0.069	0.847	1.570	3.91	bdl	0.0007	3.30	31.8
N331	515526	4048255	0.19	0.099	0.907	1.025	4.67	bdl	0.0005	0.65	30.0
N332	515484	4048245	0.49	0.041	0.717	1.986	3.38	bdl	0.0006	0.50	29.0
N334	515452	4048158	0.19	0.132	2.133	0.675	3.53	0.002	0.0004	3.50	27.8
N335	515486	4048116	0.24	0.085	2.210	0.455	4.15	0.009	0.0005	6.25	33.5
N336	515510	4048081	13.7	0.055	1.812	14.620	0.75	bdl	0.0005	0.28	25.5
N337	515504	4048034	0.056	0.020	0.400	0.352	3.28	bdl	0.0014	8.66	32.0
N338	515473	4048051	0.10	0.034	0.597	0.308	4.10	bdl	0.0005	7.66	33.9
N339	515476	4048008	0.10	0.033	0.751	0.373	4.16	bdl	0.0003	12.43	32.3
N340	515442	4048027	0.31	0.067	1.680	1.502	3.40	bdl	0.0005	14.50	31.9
N341	515444	4048067	0.25	0.039	0.615	1.095	3.07	bdl	0.0005	6.79	31.9
N342	515431	4048111	0.48	0.010	0.124	0.843	4.08	bdl	0.0004	6.16	34.2
N343	515418	4048135	1.15	0.040	0.409	0.825	3.26	0.066	bdl	6.76	31.2
N344	514870	4047612	0.64	0.012	0.194	2.015	2.61	0.038	0.16	26.36	42.8
N345	514849	4047608	0.49	0.065	0.320	0.501	3.41	0.044	0.077	12.06	51.3
N346	514830	4047587	0.12	0.025	0.605	2.853	0.98	0.33	0.48	39.57	56.8
N347	514847	4047594	0.72	0.010	0.138	2.454	3.37	0.004	0.054	17.16	42.9
N348	514857	4047579	0.36	0.008	0.426	1.658	1.34	0.72	0.28	27.30	56.9
N349	514866	4047588	2.75	0.015	0.953	0.475	2.24	bdl	0.009	8.08	43.4
N350	514841	4047574	0.33	0.012	0.675	2.538	0.85	bdl	0.27	20.88	58.1
N351	514849	4047568	0.64	0.010	0.298	4.228	0.72	1.76	0.69	36.59	62.8
N352	514868	4047562	6.93	0.011	0.665	7.972	0.71	7.16	1.91	74.48	51.7
N353	514881	4047577	9.00	0.009	0.241	1.968	0.80	bdl	0.094	6.63	51.8

Sites 1 and Mandraki are background sites outside the Lakki caldera. n.d. = not determined; n.m. = not measured; bdl = below detection limit (<0.002 for H_2S; <0.0002 for CH_4). Easting (E) and northing (N) are expressed as UTM coordinates WGS84, all sites belonging to sector 35S. Data of S concentrations and pH of samples from 1 to 17 and from N-St-1 to N-St-28 are taken from [24]. *Samples collected close to the plants of Table 3.

population (2.11-57 ppm, 43.5% of the data) indicating a significant H_2S input into the atmosphere; D population (1.5% of the data) includes values > 57 ppm of H_2S up to saturation of the sensor in the vicinity of the active fumaroles, suggesting a significant contribution of the hydrothermal fluids released from the subsurface.

Three distinct populations can be recognized (A < 8.5, B from 8.5 to 44.9, and C up to 7132 ng/m^3; 12.2%, 82.8%, and 5.0%, respectively) for GEM concentrations in the air (Figure 3(c)) that were measured with the Lumex® instrumentation.

In Figure 4, an example of H_2S, CO_2, and GEM concentrations measured in the atmosphere through transect walk within the Lakki Plain is shown. GEM, H_2S, and CO_2 concentration peaks, in correspondence with the fumaroles of Phlegeton, show a good match, confirming the interdependence of these gaseous compounds and their common origin from the fumaroles. The main fumarolic emissions were clearly highlighted by anomalously high Hg concentrations (up to ~600 ng/m^3) with respect to the surrounding air masses (~30 ng/m^3). GEM concentrations above background values measured away from the main fumarolic vents were probably due to soil degassing. The Lakki Plain and especially the main hydrothermal craters are sites of strong hydrothermal degassing with CO_2 fluxes up to 6175 g/m^2/day [52]. Mercury fluxes from the soil have not

Table 3: Hg and S concentrations in plant leaves collected in the Lakki Pain, Nisyros.

ID	Erica		ID	Cistus	
	Total Hg (μg/g)	Total S (μg/g)		Total Hg (μg/g)	Total S (μg/g)
1 NY-E	0.026	1180	1 NY-C	0.010	1080
2 NY-E	0.046	6340	2 NY-C	0.037	5950
3 NY-E	0.028	2210	3 NY-C	0.022	2420
4 NY-E	0.014	2310			
5 NY-E	0.025	1410	5 NY-C	0.055	2550
6 NY-E	0.019	1540	6 NY-C	0.019	2290
7 NY-E	0.016	2840	7 NY-C	0.056	5290
8 NY-E	0.066	2560	8 NY-C	0.112	3350
9 NY-E	0.036	3630			
10 NY-E	0.023	4360			
11 NY-E	0.039	4280	11 NY-C	0.025	3570
12 NY-E	0.030	1480	12 NY-C	0.028	2430
13 NY-E	0.036	2960	13 NY-C	0.095	4260
14 NY-E	0.065	2640	14 NY-C	0.027	2340
15 NY-E	0.024	2110	15 NY-C	0.029	2860
16 NY-E	0.023	2540	16 NY-C	0.077	3610
17 NY-E	0.034	1460	17 NY-C	0.112	3140

Soil samples identified with the numbers from 1 to 17 in Table 2 were collected close to the plant samples with the above corresponding numbers.

Table 4: Total gaseous mercury (TGM) concentrations in fumarolic gases.

Area	TGM (ng/m^3)	References
Fumaroles Japan (>100 sites)	1400-1,828,000	[36, 45, 46]
Kilauea, Hawaii (U.S.A.)	274-1031	[47]
Colima volcano (Mexico)	470-1442	[47]
White Island, New Zealand (fumarole 3)	22,000-38,000	[48]
Yellowstone caldera, U.S.A. (9 fumaroles)	415-30,000	[3]
Solfatara di Pozzuoli, Italy (fumarole BG)	93,500	[49]
Nisyros, Greece	10,500-46,300	This study

Table 5: Atmospheric Hg concentrations, Hg/S and Hg/CO_2 ratios, and total Hg outputs of fumarolic fields at closed-conduit volcanic systems.

Area	Hg atmosphere (ng/m^3)	Hg/S ($\times 10^{-6}$)	Hg/CO_2 ($\times 10^{-8}$)	Total Hg output (kg/a)	References
Las Pailas, Rincon de la Vieja, Costa Rica	n.r.	8.4	0.14-1.7	0.8-2.4	[4]
Las Hornillas, Miravalles volcano, Costa Rica	n.r.	2.01	0.35-10	4-12	[4]
Poas, Costa Rica	n.r.	0.03	n.r.	1.6-2	[4]
Tatun volcanic field, Taiwan	5.5-292	2.4-5	4-40	5-50	[71]
La Fossa crater, Vulcano, Italy	4.8-339	0.48-1.3	6 ± 0.3	0.4-7	[72]
Yellowstone caldera, U.S.A.	n.r.	n.r.	0.16-0.26	15-56	[3]
Mt. Lassen fumaroles, Cascades, U.S.A.	n.r.	n.r.	2-22	96-167	[3]
Solfatara di Pozzuoli, Italy	n.r.	n.r.	1.3	7	[49]
Solfatara di Pozzuoli, Italy	n.r.	n.r.	1.34	2	[54]
La Soufriere, Guadeloupe, Lesser Antilles	15-189	3.2	n.r.	0.8	[73]
Nea Kameni, Greece	4.5-121	n.r.	0.1-0.34	0.2-2	[53]
White Island, New Zealand	73-89	0.13-0.25	1.43-2.47	n.r.	[48]ß
Nisyros, Greece (fumaroles)	n.a.	0.03-0.16	0.76-3.5	0.7	This study
Nisyros, Greece (atmosphere: Au traps)	9.4-420	n.a.	n.a.	n.a.	This study
Nisyros, Greece (atmosphere: Lumex®)	2-7132	11-68	1.5-8.2	1.9	This study

n.r. = not reported; n.a. = not applicable.

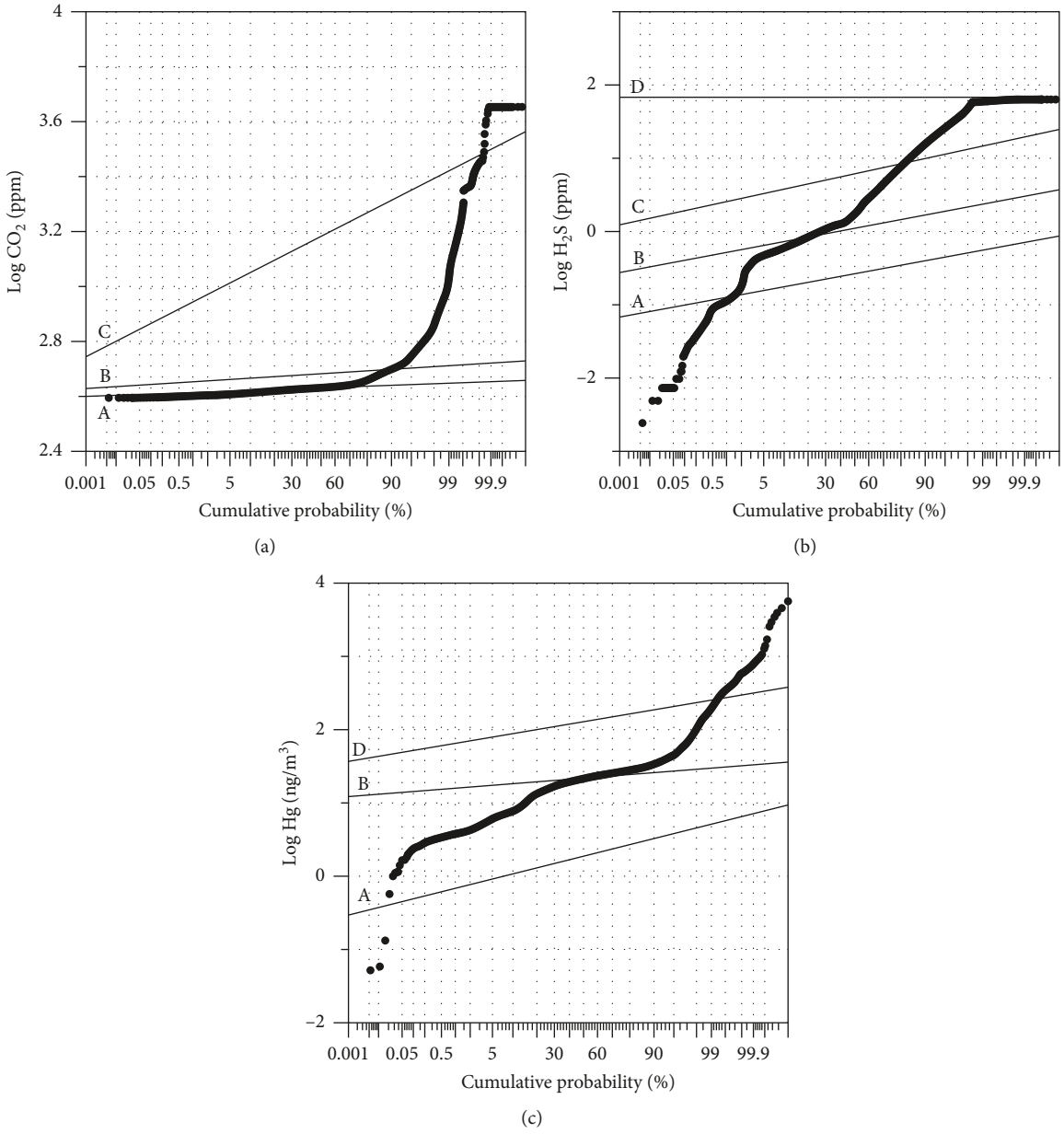


Figure 3: Probability plots of CO_2 (a), H_2S (b), and GEM (c) concentrations in the atmosphere of the Lakki Plain.

been measured at Nisyros, but as reported from the literature [3, 49, 53, 54], soils at geothermal and hydrothermal systems also emit gaseous Hg. Nevertheless, the previous authors found Hg fluxes (1-2000 μg/m^2/day) that are many orders of magnitude lower than those of CO_2, with the latter gas often acting as carrier for Hg.

5.3. Mercury in the Soil. The soils of the Lakki Plain are strongly weathered by past and present fumarolic activity. This can be recognized by the widespread presence of secondary alteration minerals, mainly sulfates [24, 25]. The main drivers of the alteration process are fumarolic H_2O and H_2S. The former is the main carrier of thermal energy, which is reflected in soil temperatures reaching up to the boiling temperature of water. Soil temperatures provide indications regarding the hydrothermal uprising gases, allowing the identification of the actively degassing areas. High temperatures are to be considered related to both high fluxes of hydrothermal fluids and the enrichment of the hydrothermal component in the soil gases. The temperature distribution map at 20 cm depth indicates temperatures above 30°C in all the investigated sites, except for some points along the western flank of the Kaminakia crater (Figure 5(a)). Higher temperatures, from 50 to 100°C, were recorded at the southern part of the Stefanos crater, at Phlegeton and Mikros Polybotes (Figure 5(a)).

Hydrogen sulphide in the fumarolic gases of Nisyros is the third most abundant species after H_2O and CO_2 [22].

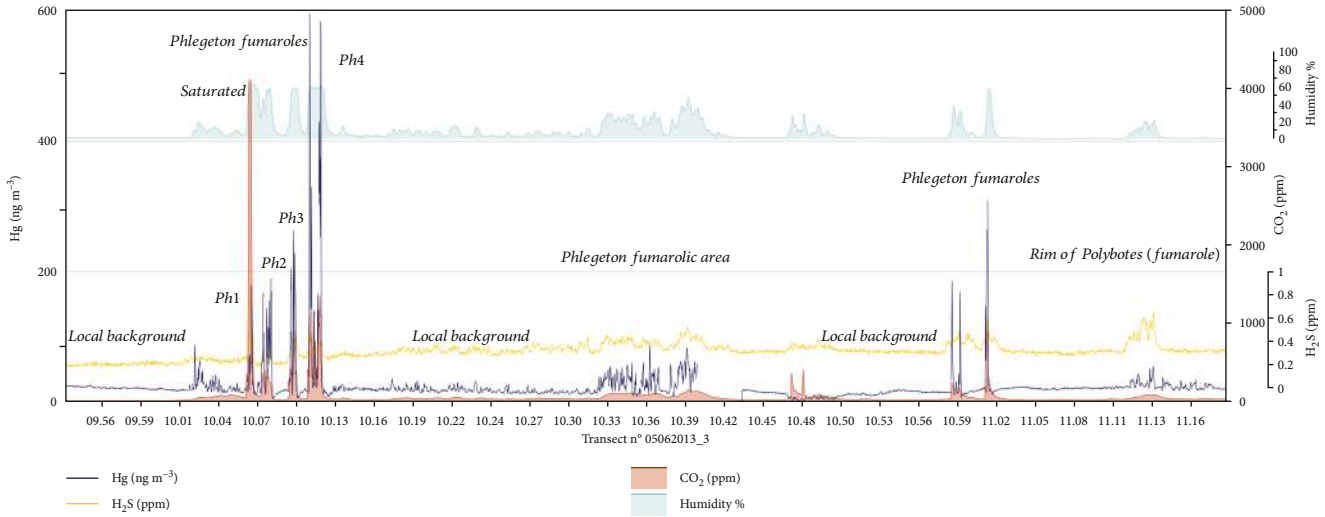


FIGURE 4: Concentrations in the atmosphere of H_2S, CO_2, and GEM measured through a transect walk inside the Lakki Plain and close to the main fumaroles (Ph = Phlegeton).

In the soil gases, on a dry basis, it represents up to nearly 18% vol. Within the soil, H_2S is oxidised by atmospheric O_2 forming sulfuric acid [55, 56], by the net reaction

$$H_2S + 2O_2 \rightarrow H_2SO_4 \quad (1)$$

Such reaction is responsible for the high S contents of the analysed soils (median ~2%, max ~56% (Table 2)) and the very low values of soil pH (from 0.71 to 5.55 (Table 2)). Both parameters show an inverse relationship (Figure 6(a)) indicating that, at the most actively exhaling zones, more sulfuric acid is produced and more sulfur is deposited.

The total amount of Hg trapped in the soil was plotted in a probability plot. As for the Hg concentrations in the air, three populations were detected (Figure 7); a secondary population containing the higher values was detected as indicated by the black arrow in Figure 7. High Hg concentrations were measured in the soil close to the main fumarolic vents (Figure 5(b)). As for sulfur, the inverse relationship between soil Hg and soil pH (Figure 6(b)) supports the transport and the deposition of Hg by fumarolic fluids. Daskalopoulou et al. [24] evidenced that also other volatile elements like As, Bi, Pb, Sb, Se, and Te are enriched in the soils of the Lakki Plain that are mostly affected by hydrothermal gases.

The accumulation of Hg in the soil matrix does not depend solely on the amount of Hg carried by the uprising hydrothermal gases but also on the soil retention capacity. Many studies demonstrated that Hg in soils shows generally a good correlation with soil organic matter (SOM). Ottesen et al. [57] evidenced such positive correlation at the continental scale, based on the analysis of more than 4000 soil samples from 33 countries in Europe. Martin et al. [58] found that the same correlation holds true for the volcanic soils of Mt. Etna. Elemental carbon, which can be considered a proxy for SOM, in the soils of the Lakki Plain does not show any correlation with the measured Hg values. This probably depends on the fact that most of the sampled soils are totally devoid of vegetation, limiting the presence of SOM to some vegetal debris and microbial communities. The low content of SOM may therefore not contribute much to Hg accumulation in the soils of the Lakki Plain. Sulphide, which could also react with Hg, is also very scarce in the surface soil levels due to the oxidising environment [24].

Soil temperatures are thought to play an important role in Hg retention in soils. This parameter has probably a contrasting effect because higher soil temperatures indicate stronger hydrothermal gases transporting more Hg from the depth, but at the same time, higher soil temperatures presuppose also a faster remobilization of Hg from the soils because of its high volatility [3].

Although hydrothermal gases like CO_2 and H_2S show their maxima close to the main fumarolic areas (Figures 5(d) and 5(e)), no correlation with soil Hg could be evidenced (p value 0.77 and 0.83, respectively, and correlation index 0.04 and 0.02, respectively). However, even though both soil and gas samples were collected at the same time and in the same place, they are not totally comparable as CO_2 and H_2S were measured on the gas phase collected at the 50 cm depth while Hg was measured on the solid phase at the soil surface. Nevertheless, a better correlation was expected.

5.4. Mercury in the Plants. Plant leaves present lower concentrations with respect to the soils where they grow, while the local background in both plant leaves and soils shows very low concentrations in total Hg. Results show a range of values regarding the total Hg concentrations that seem to be positively correlated with the intensity of the fumarolic activity. The highest concentrations were measured in sites located close to the hydrothermal drill and the craters of Stefanos, Phlegeton, Mikros Polybotes, and Kaminakia, confirming the impact of the hydrothermal activity on the surrounding environment.

Regarding the availability of soil Hg to plants, it is considered to be low as there is a tendency for Hg to accumulate in

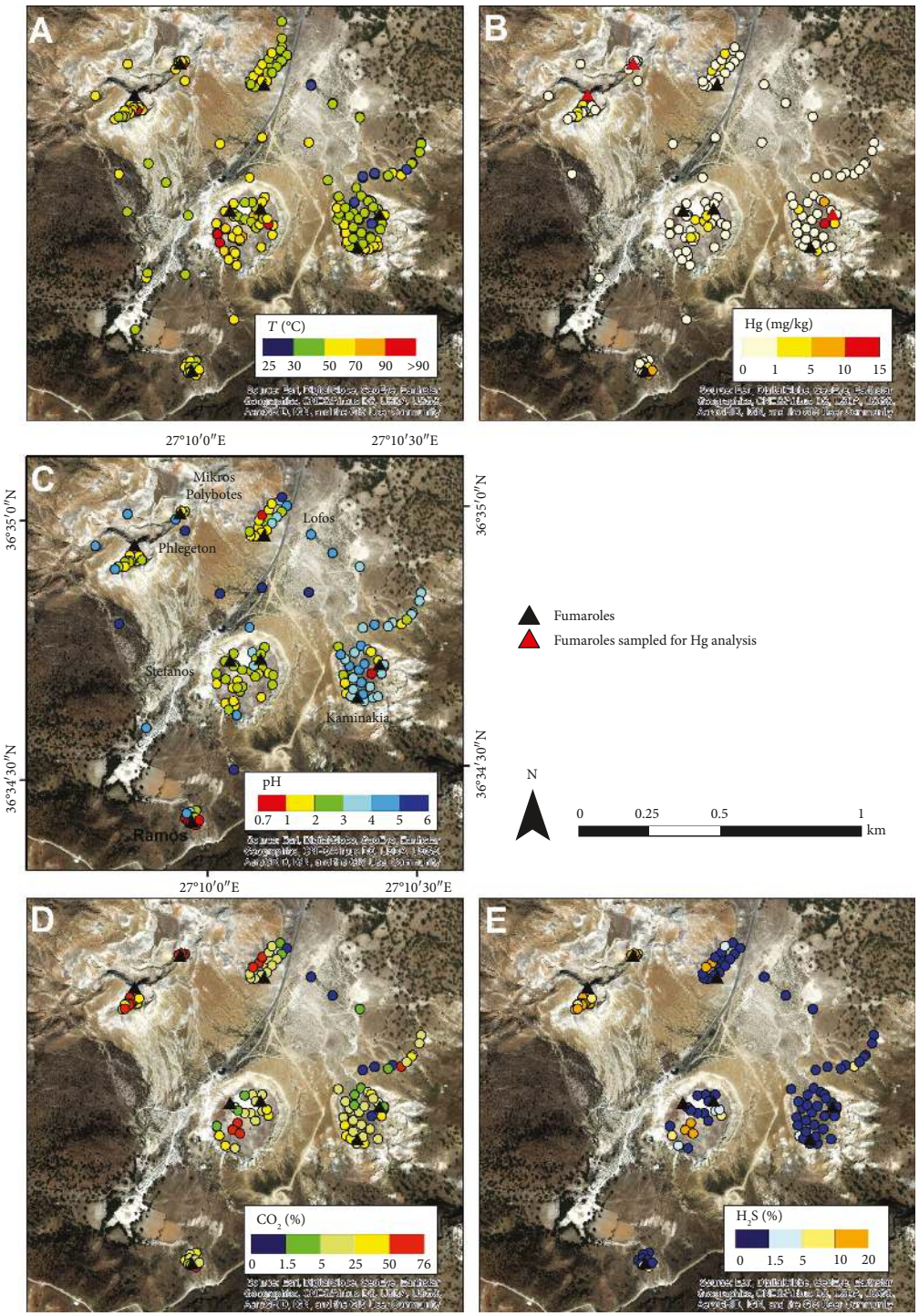


FIGURE 5: Distribution maps of soil temperature (a), Hg soil concentrations (b), soil pH (c), soil CO_2 (d), and H_2S (e) concentrations in the Lakki Plain area.

the roots, indicating that the roots serve as a barrier to Hg uptake [59, 60]. Mercury concentration in aboveground parts of plants appears to depend largely on foliar uptake of Hg^0 volatilized from the soil [61, 62] and therefore on the age of the plant and the time of day and year [63]. The transfer of Hg (gaseous forms) from the atmosphere occurs by dry and wet deposition (rain and snow) and enters into the organism by the stomata of the leaves through the transpiration process [59, 61, 64, 65]. The soil-plant correlation diagram (Figures 8(a) and 8(b)) shows that *Cistus* samples were enriched in Hg with respect to *Erica* presenting a moderately good positive correlation.

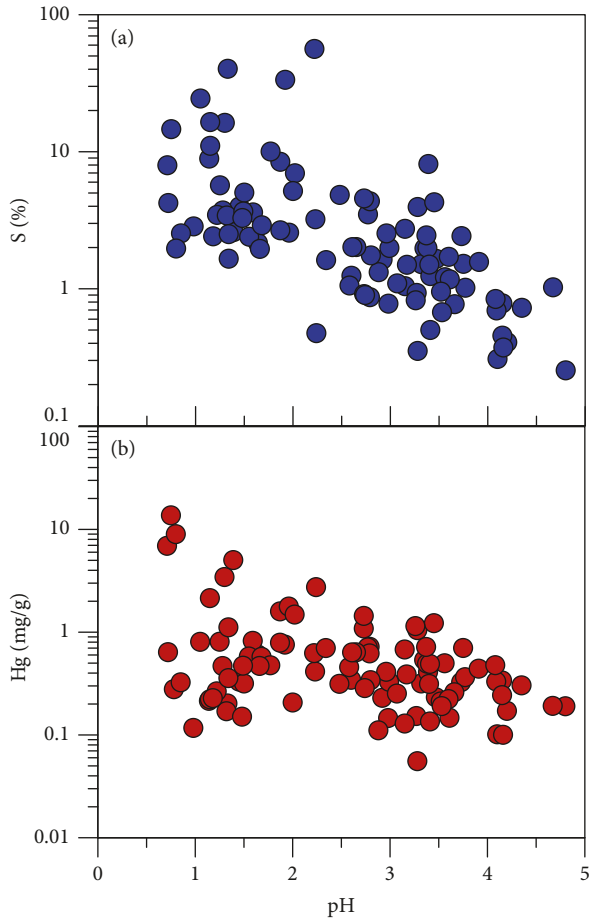


Figure 6: Soil total sulfur (a) and total Hg (b) concentrations vs. soil pH binary diagrams.

Taking into consideration that Hg uptake is mostly through the leaves and the samples of both species were collected on the same day, the relatively high concentrations of total Hg in the *Cistus* samples can be justified by the higher specific surface area of its leaflets with respect to *Erica*'s. Additionally, equally important factors that should be taken into consideration are the solar radiation and the humidity. These two factors along with the specific surface area of the leaflets may possibly explain the elevated Hg concentration of the local background sample that was noticed at Erica. It is worth mentioning that the local background samples of both species were collected at a place located close to the sea, at noontime during summer period.

On the other hand, sulfur is an essential macronutrient for plant growth. Its uptake and distribution are tightly controlled by the environmentally induced changes in nutrient demand [66, 67]. Therefore, the high concentrations in S as well as the good correlation between the soil and plant samples in both species can be regarded as mainly caused by its uptake by the roots through the metabolic processes of the plants (Figures 8(c) and 8(d)). Nevertheless, the contribution of the transpiration process via the stomata of the leaves may also be important.

5.5. Environmental and Human Health Issues. Mercury is considered to be among the most toxic metals that could be taken by the human body through different pathways [13], especially concerning methylated species. Furthermore, its deleterious effects can be enhanced through its biomagnification along the trophic chain [11]. One of the primary uptake paths of Hg is through the inhalation of GEM. For the World Health Organization [68], atmospheric concentrations of Hg in the range of 15,000–30,000 ng/m^3 may have adverse effects on humans (tremors, renal tubular effects, change in plasma enzymes, and others). However, using an uncertainty factor of 20, the same organization proposed a guideline value for Hg concentration in air of 1000 ng/m^3 [68].

At the same time, the US Occupational Safety and Health Administration considered a permissible occupational exposure limit for GEM of 100,000 ng/m^3 in the air [69], while the National (US) Institute for Occupational Safety and Health (NIOSH) established a recommended exposure limit for GEM of 50,000 ng/m^3 as a time-weighted average (TWA) for up to a 10 h workday and a 40 h workweek [69]. The American Conference of Governmental Industrial Hygienists assigned to GEM a threshold limit value of 25,000 ng/m^3 as a TWA for a normal 8 h workday and a 40 h workweek [69]. The minimum risk level (MRL) for chronic inhalation of GEM is 200 ng/m^3 [69, 70]. The MRL is an estimate of the daily human exposure to a hazardous substance that is likely to be without appreciable risk of adverse health effects over a specified duration of exposure. The US EPA reference concentration for inhalation is calculated to be 300 ng/m^3 (TWA) [69].

Taking into consideration the above limits and thresholds, it may be deduced that, although the atmospheric GEM concentrations within the Nisyros Caldera are sometimes many orders of magnitude above the global background, they do not represent a general hazard for human health. The area is yearly visited by many tens of thousands of tourists, but the zones where they arrive show GEM concentrations rarely exceeding the MRL. Areas exceeding the WHO guideline value of 1000 ng/m^3 are very close to the main fumarolic vents where tourists are not allowed to go and where other toxic gases of higher danger are present (i.e., H_2S [19]). Moreover, people who work all day in the area (ticket operators, owner, and employees of the Volcano Café) spend most of their time in areas with atmospheric GEM concentrations well below the occupational limits and generally also below the MRL. Probably, only volcanologists that take gas samples from the main fumaroles may be exposed to atmospheric GEM levels of a few thousands of ng/m^3 for some hour, which has still to be considered a low exposition. Even though results propose no particular risk, a more complete survey is highly suggested to have a more accurate picture.

5.6. Total Output from the Hydrothermal System of Nisyros. It has long been established that the contribution of volcanic activity to the total natural emissions of Hg to the atmosphere is substantial [2, 4, 47]. However, due to the limited number of data available, significant uncertainties on the annual emissions of volcanic Hg still remain. Estimates range

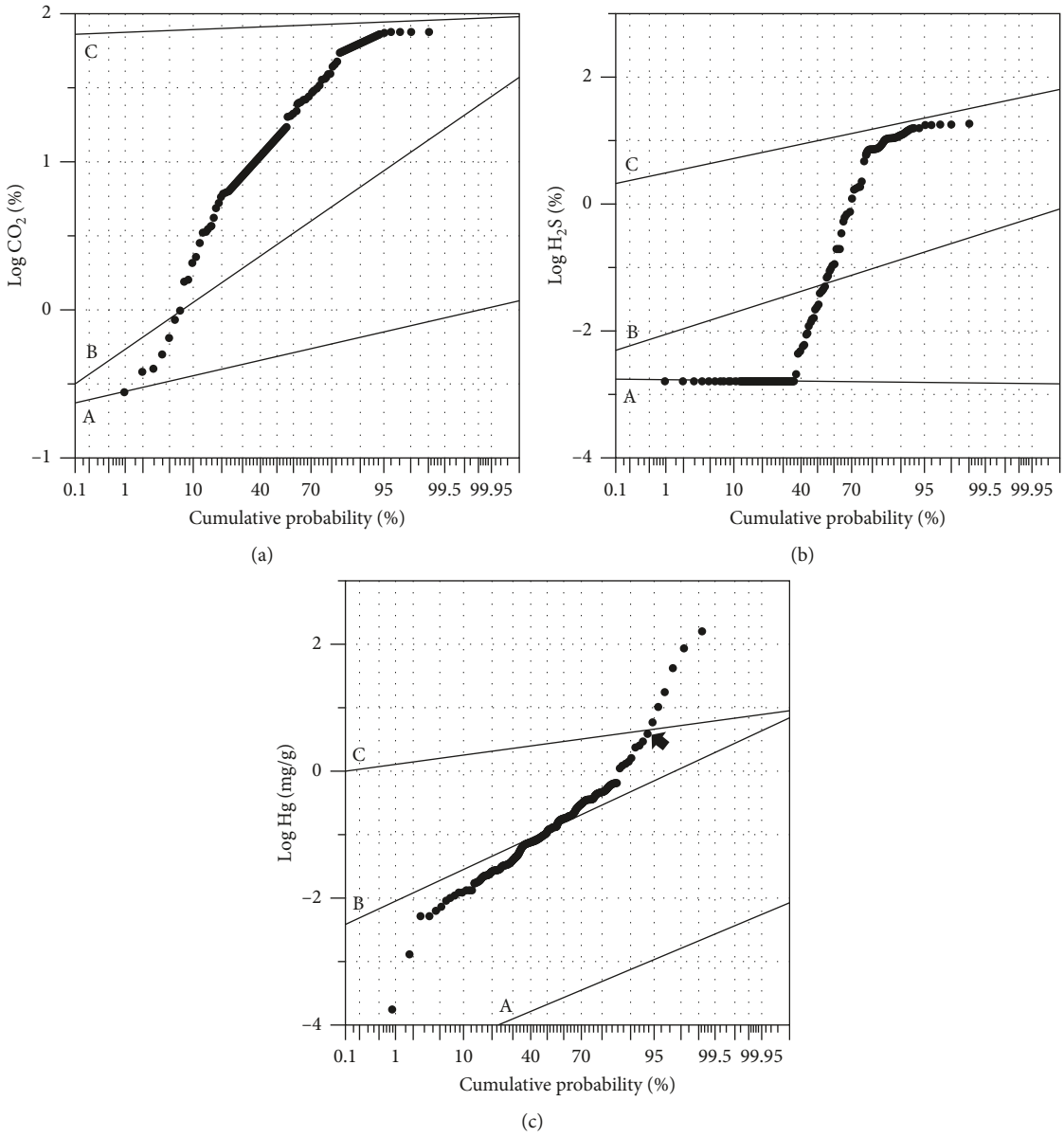


Figure 7: Probability plots of total CO_2 (a) and H_2S (b) concentrations in the soil gas and Hg (c) concentrations in the soils of the Lakki Plain.

between 0.6 and 1000 t/a representing a proportion that varies from <1% up to 50% of total natural emissions [2, 4, and references therein]. The strongest contribution (90%) of the total output of volcanic Hg derives from explosive eruptions while the rest derives from passive degassing [2]. Emissions of single open-conduit volcanoes like Etna (Italy), Ambrim (Vanuatu), or Masaya (Nicaragua) are in the order of units to tens of t/a [4], pointing to strong underestimation of global volcanic outputs lower than 50 t/a. The contribution of fumarolic emissions from closed-conduit volcanoes is instead very limited as it is found in the range from 0.2 to 167 kg/a (0.0002-0.167 t/a (Table 5)).

Most of the Hg flux estimations from volcanic systems have been indirectly obtained cross-correlating the measured SO_2 fluxes with the Hg/SO_2 ratios measured in the volcanic plume [4]. Such method cannot be used for low-temperature fumarolic areas because magmatic SO_2 is strongly scrubbed by the hydrothermal system. To obtain output estimates for such areas, different methods have been proposed. One of which is the measurement of Hg fluxes from the soils with accumulation chambers (dynamic flux chambers or static closed chambers) and the consequent integration of the fluxes over the whole hydrothermal area. Such method was applied only few times [49, 53, 54]. Another method is the cross-correlation of the total CO_2 release of the fumarolic area with the Hg/CO_2 ratio being measured either in the fumarolic fluids or in the air close to the vents [4]. Both methods give the order of magnitude of

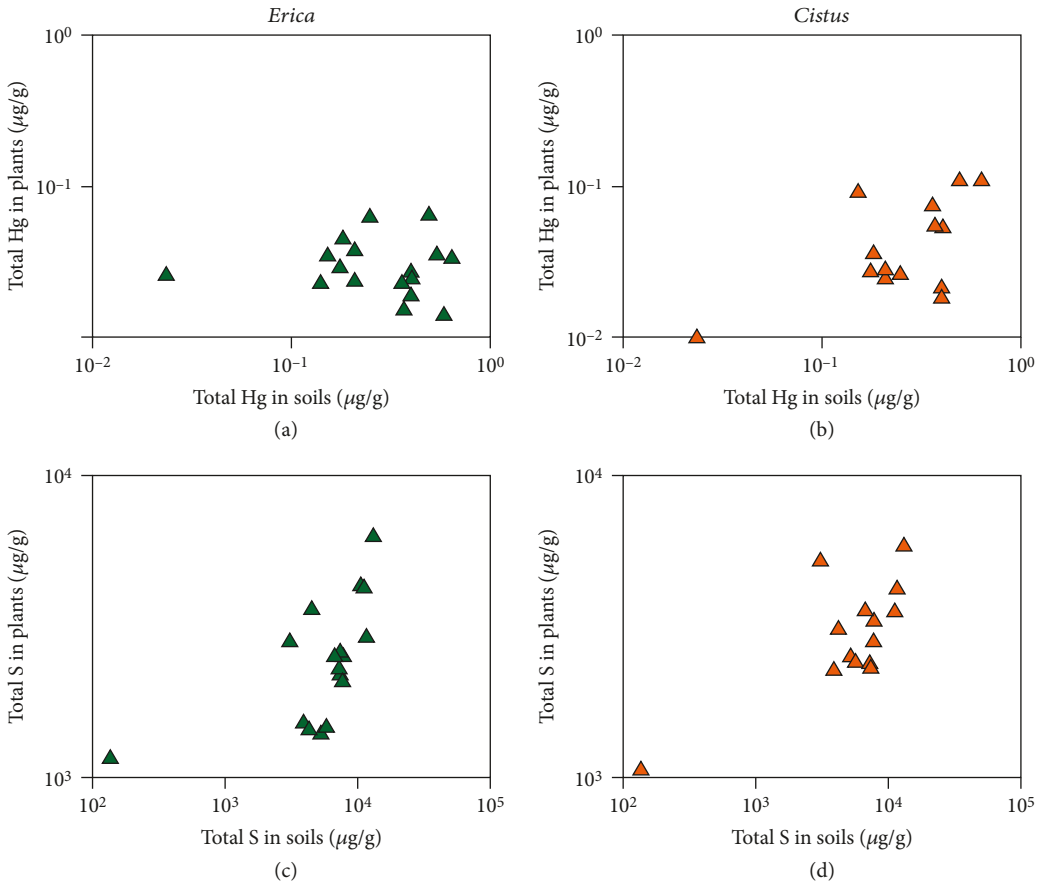


FIGURE 8: Correlation plots that present in the upper part the total Hg concentrations in soils and (a) *Erica* and (b) *Cistus* and in the lower part the total S concentrations in soils and (c) *Erica* and (d) *Cistus* collected in the Lakki Plain.

the Hg output, but they coherently confirm much lower outputs of fumarolic areas with respect to open-conduit volcanoes. Following the second approach, a rough estimation of the Hg output of Nisyros can be obtained considering the total CO_2 output, as determined by Bagnato et al. [53], which is 84 t/d, and the Hg/CO_2 ratios measured in the fumaroles that range from 0.8×10^{-8} to 3.5×10^{-8} (median value = 2.3×10^{-8}) or in the air ranging from 1.5×10^{-8} to 8.2×10^{-8} (median value = 6.3×10^{-8}), corresponding to the total Hg output of 0.7 and 1.9 kg/a, respectively. Such figures fall in the lower range of the outlet values for fumarolic areas (Table 5).

6. Conclusions

Mercury and its compounds are highly toxic for humans and ecosystems. Volcanic and hydrothermal emissions are major natural sources of Hg in the atmosphere. At Nisyros, a potentially active volcano with intense and widespread degassing activity, real-time measurements of GEM showed concentrations up to 7132 ng/m^3 within the Lakki Plain. The good correlation between Hg and the main fumarolic gases (H_2O, CO_2, and H_2S) confirms the hydrothermal origin of the former. In the fumarolic gases, Hg was estimated in the range 10,500-46,300 ng/m^3; these values should be considered the lower limit due to the plausible Hg loss within the condensing fumarolic vapour. Relatively high Hg concentrations were also identified in the soils; the accumulation of Hg in the soil matrix is dependent on both the amount carried by the upflowing hydrothermal gases and the soil ability to fix a part of it. The lack of vegetation at the crater area maybe responsible of the poor correlation between elemental C and Hg in the soil. No bioavailability through the roots was noticed in the plants collected at the Lakki Plain. The slightly high concentrations of the vegetation samples could have therefore been caused by the transpiration process that takes place in the stomata of the leaves, making *Cistus* a better candidate for biomonitoring investigations with respect to *Erica* due to the greater specific area of its leaves.

The aforementioned synoptic analysis of the results highlights that more than one matrix can be affected by hydrothermal Hg from the degassing activity. Furthermore, it underscores that Hg concentrations are positively correlated with the distance of the sample/measurement from the emission point. Even though the measured Hg concentrations were enhanced and at cases exceed the WHO limits in terms of inhalation, they seem to be of minor risk for human health as the exposure is for a limited time and the access for nonvolcanologists is prohibited. However, an uptake originating from the trophic chain should not be disregarded.

Data Availability

Data will be available on request.

Disclosure

K. Daskalopoulou's present address is GFZ-German Research Centre for Geosciences, Potsdam, Brandenburg, Germany. F. Capecchiacci's present address is Istituto Nazionale di Geofisica e Vulcanologia, Osservatorio Vesuviano, Naples, Italy. G. Giudice's present address is Istituto Nazionale di Geofisica e Vulcanologia, Osservatorio Etneo, Catania, Italy.

Conflicts of Interest

The authors declare that they have no conflicts of interest.

Acknowledgments

We are grateful to Emanuela Bagnato, who made the measurements of the Au traps at the University of Palermo, to Mario Sprovieri who allowed us to make the measurements of Hg in the soils at the laboratories of the Consiglio Nazionale delle Ricerche, IAMC, UOS di Capo Granitola, and to Jens Fiebig, Artemis Kontomichalou, and Konstantinos Kyriakopoulos for their help in the field. We kindly acknowledge the owner of the Volcano Café, Mr. Sideris Kontogiannis, for his logistical support to all volcanologists working in the Nisyros Caldera (and also for many beers spent for free and for the delightful music of his Cretan Lyra at dusk). Finally, we would like to thank the municipality of Nisyros Island for its hospitality and generosity.

References

[1] M. S. Gustin, "Are mercury emissions from geologic sources significant? A status report," *Science of The Total Environment*, vol. 304, no. 1-3, pp. 153–167, 2003.

[2] D. M. Pyle and T. A. Mather, "The importance of volcanic emissions for the global atmospheric mercury cycle," *Atmospheric Environment*, vol. 37, no. 36, pp. 5115–5124, 2003.

[3] M. A. Engle, M. S. Gustin, F. Goff et al., "Atmospheric mercury emissions from substrates and fumaroles associated with three hydrothermal systems in the western United States," *Journal of Geophysical Research*, vol. 111, no. D17, article D17304, 2006.

[4] E. Bagnato, G. Tamburello, G. Avard et al., "Mercury fluxes from volcanic and geothermal sources: an update," *Geological Society, London, Special Publications*, vol. 410, no. 1, pp. 263–285, 2015.

[5] S. Metz and J. H. Trefry, "Chemical and mineralogical influences on concentrations of trace metals in hydrothermal fluids," *Geochimica et Cosmochimica Acta*, vol. 64, no. 13, pp. 2267–2279, 2000.

[6] A. Kabata-Pendias and A. Pendias, *Trace Elements in Soils and Plants*, CRC, third ed edition, 2001.

[7] R. P. Mason, W. F. Fitzgerald, and F. M. M. Morel, "The biogeochemical cycling of elemental mercury: anthropogenic influences," *Geochimica et Cosmochimica Acta*, vol. 58, no. 15, pp. 3191–3198, 1994.

[8] C. H. Lamborg, C. M. Tseng, W. F. Fitzgerald, P. H. Balcom, and C. R. Hammerschmidt, "Determination of the mercury complexation characteristics of dissolved organic matter in natural waters with "reducible Hg" titrations," *Environmental Science & Technology*, vol. 37, no. 15, pp. 3316–3322, 2003.

[9] W. F. Fitzgerald, R. P. Mason, and G. M. Vandal, "Atmospheric cycling and air-water exchange of mercury over mid-continental lacustrine regions," *Water, Air & Soil Pollution*, vol. 56, no. 1, pp. 745–767, 1991.

[10] F. M. M. Morel, A. M. L. Kraepiel, and M. Amyot, "The chemical cycle and bioaccumulation of mercury," *Annual Review of Ecology and Systematics*, vol. 29, no. 1, pp. 543–566, 1998.

[11] W. F. Fitzgerald and C. H. Lamborg, "Geochemistry of mercury in the environment," in *Environmental Geochemistry, Treatise on Geochemistry*, H. Holland and K. Turekian, Eds., pp. 1–47, Elsevier, 2007.

[12] T. W. Clarkson and L. Magos, "The toxicology of mercury and its chemical compounds," *Critical Reviews in Toxicology*, vol. 36, no. 8, pp. 609–662, 2006.

[13] WHO, *Exposure to Mercury: A Major Public Health Concern*, World Health Organization and United Nations Environment Programme, Geneva, Switzerland, 2007.

[14] H. L. Barnes and T. M. Seward, "Geothermal systems and mercury deposits," in *Geochemistry of Hydrothermal Ore Deposits*, H. L. Barnes, Ed., pp. 699–736, John Wiley & Sons, New York, 3rd ed. edition, 1997.

[15] E. Bagnato, A. Aiuppa, F. Parello et al., "Degassing of gaseous (elemental and reactive) and particulate mercury from Mount Etna volcano (Southern Italy)," *Atmospheric Environment*, vol. 41, no. 35, pp. 7377–7388, 2007.

[16] D. A. Nimick, R. R. Caldwell, D. R. Skaar, and T. M. Selch, "Fate of geothermal mercury from Yellowstone National Park in the Madison and Missouri Rivers, USA," *Science of The Total Environment*, vol. 443, pp. 40–54, 2013.

[17] D. E. Robertson, E. A. Crecelius, J. S. Fruchter, and J. D. Ludwick, "Mercury emissions from geothermal power plants," *Science*, vol. 196, no. 4294, pp. 1094–1097, 1977.

[18] S. Vitolo and M. Seggiani, "Mercury removal from geothermal exhaust gas by sulfur-impregnated and virgin activated carbons," *Geothermics*, vol. 31, no. 4, pp. 431–442, 2002.

[19] W. D'Alessandro, L. Brusca, K. Kyriakopoulos, G. Michas, and G. Papadakis, "Hydrogen sulphide as a natural air contaminant in volcanic/geothermal areas: the case of Sousaki, Corinthia (Greece)," *Environmental Geology*, vol. 57, no. 8, pp. 1723–1728, 2009.

[20] J. Cabassi, F. Tassi, S. Venturi et al., "A new approach for the measurement of gaseous elemental mercury (GEM) and H_2S in air from anthropogenic and natural sources: examples from Mt. Amiata (Siena, Central Italy) and Solfatara Crater (Campi Flegrei, Southern Italy)," *Journal of Geochemical Exploration*, vol. 175, pp. 48–58, 2017.

[21] L. Marini and J. Fiebig, "Fluid geochemistry of the magmatic-hydrothermal system of Nisyros (Greece)," *Mémoires de Géologie (Lausanne)*, vol. 44, p. 192, 2005.

[22] J. Fiebig, F. Tassi, W. D'Alessandro, O. Vaselli, and A. B. Woodland, "Carbon-bearing gas geothermometers for volcanic-hydrothermal systems," *Chemical Geology*, vol. 351, pp. 66–75, 2013.

[23] K. Daskalopoulou, S. Calabrese, F. Grassa et al., "Origin of methane and light hydrocarbons in natural fluid emissions: a

key study from Greece," *Chemical Geology*, vol. 479, pp. 286–301, 2018.

[24] K. Daskalopoulou, S. Calabrese, S. Milazzo et al., "Trace elements mobility in soils from the hydrothermal area of Nisyros (Greece)," *Annals of Geophysics*, vol. 57, Fast Track 2, 2014.

[25] S. Venturi, F. Tassi, O. Vaselli et al., "Active hydrothermal fluids circulation triggering smallscale collapse events: the case of the 2001–2002 fissure in the Lakki Plain (Nisyros Island, Aegean Sea, Greece)," *Natural Hazards*, vol. 93, no. 2, pp. 601–626, 2018.

[26] P. Nomikou, D. Papanikolaou, and V. J. Dietrich, "Geodynamics and volcanism in the Kos-Yali-Nisyros volcanic field," in *Nisyros Volcano - The Kos - Yali - Nisyros Volcanic Field*, Series: Active Volcanoes of the World, V. J. Dietrich and E. Lagios, Eds., pp. 13–55, Springer International Publishing, 2018.

[27] J. C. Hunziker and L. Marini, *The geology, geochemistry and evolution of Nisyros Volcano (Greece). Implications for the volcanic hazards*, no. 44, 2005Memoires de Geologie (Lausanne), 2005.

[28] V. J. Dietrich, "Geology of Nisyros Volcano," in *Nisyros Volcano - The Kos - Yali - Nisyros Volcanic Field, Series: Active Volcanoes of the World*, V. J. Dietrich and E. Lagios, Eds., pp. 145–201, Springer International Publishing, 2018.

[29] V. J. Dietrich, G. Chiodini, and F. M. Schwandner, "The hydrothermal system and geothermal activity," in *Nisyros Volcano - The Kos - Yali - Nisyros Volcanic Field, Series: Active Volcanoes of the World*, V. J. Dietrich and E. Lagios, Eds., pp. 57–102, Springer International Publishing, 2018.

[30] T. Brombach, S. Caliro, G. Chiodini, J. Fiebig, J. C. Hunziker, and B. Raco, "Geochemical evidence for mixing of magmatic fluids with seawater, Nisyros hydrothermal system, Greece," *Bulletin of Volcanology*, vol. 65, no. 7, pp. 505–516, 2003.

[31] S. Caliro, G. Chiodini, D. Galluzzo et al., "Recent activity of Nisyros volcano (Greece) inferred from structural, geochemical and seismological data," *Bulletin of Volcanology*, vol. 67, no. 4, pp. 358–369, 2005.

[32] W. D'Alessandro, A. L. Gagliano, K. Kyriakopoulos, and F. Parello, "Hydrothermal methane fluxes from the soil at Lakki plain (Nisyros, Greece)," in *Proceedings of the 13th International Congress of the Geological Society of Greece*, vol. 47no. 3, pp. 1920–1928, Chania, Crete, Greece, September 2013, Bulletin of the Geological Society of Greece.

[33] US EPA, "Method 7473 (SW-846): mercury in solids and solutions by thermal decomposition, amalgamation, and atomic absorption spectrophotometry," 1998, February 2019, https://www.epa.gov/sites/production/files/2015-07/documents/epa-7473.pdf.

[34] G. W. Thomas, "Soil pH and soil acidity," in *Methods of soil analysis – Part 3 Chemical methods*, Book Series, D. L. Sparks, Ed., no. 5pp. 475–490, Soil Sci. Soc. Am, 1996.

[35] R. Ebinghaus, S. G. Jennings, W. H. Schroeder et al., "International field intercomparison measurements of atmospheric mercury species at Mace head, Ireland," *Atmospheric Environment*, vol. 33, no. 18, pp. 3063–3073, 1999.

[36] R. Nakagawa, "Estimation of mercury emissions from geothermal activity in Japan," *Chemosphere*, vol. 38, no. 8, pp. 1867–1871, 1999.

[37] US EPA, *Method IO-5: Sampling and Analysis for Atmospheric Mercury. Compendium of Methods for the Determination of Inorganic Compounds in Ambient Air*, Center for Environmental Research Information Office of Research and Development, US Environmental Protection Agency, Cincinnati, OH, 1999.

[38] S. E. Sholupov and A. A. Ganeyev, "Zeeman atomic absorption spectrometry using high frequency modulated light polarization," *Spectrochimica Acta Part B: Atomic Spectroscopy*, vol. 50, no. 10, pp. 1227–1236, 1995.

[39] S. Sholupov, S. Pogarev, V. Ryzhov, N. Mashyanov, and A. Stroganov, "Zeeman atomic absorption spectrometer RA-915+ for direct determination of mercury in air and complex matrix samples," *Fuel Processing Technology*, vol. 85, no. 6-7, pp. 473–485, 2004.

[40] A. Aiuppa, C. Federico, G. Giudice, and S. Gurrieri, "Chemical mapping of a fumarolic field: La Fossa Crater, Vulcano Island (Aeolian Islands, Italy)," *Geophysical Research Letters*, vol. 32, no. 13, article L13309, 2005.

[41] G. Tamburello, "Ratiocalc: software for processing data from multicomponent volcanic gas analyzers," *Computers & Geosciences*, vol. 82, pp. 63–67, 2015.

[42] A. J. Sinclair, "Selection of threshold values in geochemical data using probability graphs," *Journal of Geochemical Exploration*, vol. 3, no. 2, pp. 129–149, 1974.

[43] W. D'Alessandro, A. Aiuppa, S. Bellomo et al., "Sulphur-gas concentrations in volcanic and geothermal areas in Italy and Greece: characterising potential human exposures and risks," *Journal of Geochemical Exploration*, vol. 131, pp. 1–13, 2013.

[44] J. Fiebig, S. Hofmann, F. Tassi, W. D'Alessandro, O. Vaselli, and A. B. Woodland, "Isotopic patterns of hydrothermal hydrocarbons emitted from Mediterranean volcanoes," *Chemical Geology*, vol. 396, pp. 152–163, 2015.

[45] R. Nakagawa, "Amounts of mercury discharged to atmosphere from fumaroles and hot spring gases in geothermal areas," *Nippon Kagaku Kaishi*, vol. 1984, no. 5, pp. 709–715, 1984.

[46] R. Nakagawa, "Amounts of mercury discharged to atmosphere from fumaroles in geothermal areas of Hokkaido," *Nippon Kagaku Kaishi*, vol. 1985, no. 4, pp. 703–708, 1985.

[47] J. C. Varekamp and P. R. Buseck, "Global mercury flux from volcanic and geothermal sources," *Applied Geochemistry*, vol. 1, no. 1, pp. 65–73, 1986.

[48] B. W. Christenson and E. K. Mroczek, "Potential reaction pathways of Hg in some New Zealand hydrothermal environments," in *Volcanic, Geothermal, and Ore-Forming Fluids: Rulers and Witnesses of Processes within the Earth*, S. F. Simmons and I. Graham, Eds., vol. 10, pp. 111–132, Spec. Publ. Soc. Economic Geologists, 2003.

[49] E. Bagnato, F. Parello, M. Valenza, and S. Caliro, "Mercury content and speciation in the Phlegrean Fields volcanic complex: evidence from hydrothermal system and fumaroles," *Journal of Volcanology and Geothermal Research*, vol. 187, no. 3-4, pp. 250–260, 2009.

[50] N. Pirrone, S. Cinnirella, A. Dastoor et al., "Atmospheric pathways, transport and fate," *Technical Background Report for the Global Mercury Assessment 2013*, AMAP/UNEP. Arctic Monitoring and Assessment Programme, Oslo, Norway/UNEP Chemicals Branch, Geneva, Switzerland, 2013.

[51] NOAA-ESRL, "National Oceanic & Atmospheric Administration – Earth System Research Laboratory – Global Monitoring Division," 2019, February 2019, ftp://aftp.cmdl.noaa.gov/products/trends/co2/co2_annmean_gl.txt.

[52] C. Cardellini, G. Chiodini, and F. Frondini, "Application of stochastic simulation to CO_2 flux from soil: mapping and quantification of gas release," *Journal of Geophysical Research*, vol. 108, no. B9, article 2425, 2003.

[53] E. Bagnato, G. Tamburello, A. Aiuppa, M. Sprovieri, G. E. Vougioukalakis, and M. Parks, "Mercury emissions from soils and fumaroles of Nea Kameni volcanic centre, Santorini (Greece)," *Geochemical Journal*, vol. 47, no. 4, pp. 437–450, 2013.

[54] F. Tassi, J. Cabassi, S. Calabrese et al., "Diffuse soil gas emissions of gaseous elemental mercury (GEM) from hydrothermal-volcanic systems: an innovative approach by using the static closed-chamber method," *Applied Geochemistry*, vol. 66, pp. 234–241, 2016.

[55] V. W. Lueth, R. O. Rye, and L. Peters, ""Sour gas" hydrothermal jarosite: ancient to modern acid-sulfate mineralization in the southern Rio Grande Rift," *Chemical Geology*, vol. 215, no. 1-4, pp. 339–360, 2005.

[56] D. R. Zimbelman, R. O. Rye, and G. N. Breit, "Origin of secondary sulfate minerals on active andesitic stratovolcanoes," *Chemical Geology*, vol. 215, no. 1-4, pp. 37–60, 2005.

[57] R. T. Ottesen, M. Birke, T. E. Finne et al., "Mercury in European agricultural and grazing land soils," *Applied Geochemistry*, vol. 33, pp. 1–12, 2013.

[58] R. S. Martin, M. L. I. Witt, G. M. Sawyer et al., "Bioindication of volcanic mercury (Hg) deposition around Mt. Etna (Sicily)," *Chemical Geology*, vol. 310-311, pp. 12–22, 2012.

[59] M. Lodenius, "Use of plants for biomonitoring of airborne mercury in contaminated areas," *Environmental Research*, vol. 125, pp. 113–123, 2013.

[60] A. Pérez-Sanz, R. Millán, M. J. Sierra et al., "Mercury uptake by *Silene vulgaris* grown on contaminated spiked soils," *Journal of Environmental Management*, vol. 95, no. 2012, pp. S233–S237, 2012.

[61] L. Fay and M. S. Gustin, "Investigation of mercury accumulation in cattails growing in constructed wetland mesocosms," *Wetlands*, vol. 27, no. 4, pp. 1056–1065, 2007.

[62] L. Windham-Myers, J. A. Fleck, J. T. Ackerman et al., "Mercury cycling in agricultural and managed wetlands: a synthesis of methylmercury production, hydrologic export, and bioaccumulation from an integrated field study," *Science of the Total Environment*, vol. 484, no. 1, pp. 221–231, 2014.

[63] M. D. Tabatchnick, G. Nogaro, and C. R. Hammerschmidt, "Potential sources of methylmercury in tree foliage," *Environmental Pollution*, vol. 160, no. 1, pp. 82–87, 2012.

[64] L. Poissant, H. H. Zhang, J. Canário, and P. Constant, "Critical review of mercury fates and contamination in the Arctic tundra ecosystem," *Science of the Total Environment*, vol. 400, no. 1-3, pp. 173–211, 2008.

[65] A. Adjorlolo-Gasokpoh, A. A. Golow, and J. Kambo-Dorsa, "Mercury in the surface soil and cassava, *Manihot esculenta* (flesh, leaves and peel) near goldmines at Bogoso and Prestea, Ghana," *Bulletin of Environmental Contamination and Toxicology*, vol. 89, no. 6, pp. 1106–1110, 2012.

[66] N. Yoshimoto, E. Inoue, K. Saito, T. Yamaya, and H. Takahashi, "Phloem-localizing sulfate transporter, Sultr1;3, mediates re-distribution of sulfur from source to sink organs in *Arabidopsis*," *Plant Physiology*, vol. 131, no. 4, pp. 1511–1517, 2003.

[67] P. Buchner, C. E. E. Stuiver, S. Westerman et al., "Regulation of sulfate uptake and expression of sulfate transporter genes in *Brassica oleracea* as affected by atmospheric H_2S and pedospheric sulfate nutrition," *Plant Physiology*, vol. 136, no. 2, pp. 3396–3408, 2004.

[68] WHO, *Air quality guidelines for Europe. WHO Regional Publications European Series 91*, World Health Organization Regional Office for Europe, Copenhagen, 2000.

[69] US OSHA, "Health and safety (Hg). Occupational Hazards," 2007, March 2018, https://www.osha.gov/SLTC/mercury/index.html.

[70] EPA/ATSDR, "National Mercury Cleanup Policy Workgroup: action levels for elemental mercury spills," 2012, February 2019, http://www.atsdr.cdc.gov/emergency_response/Action_Levels_for_Elemental_Mercury_Spills_2012.pdf.

[71] M. L. I. Witt, T. P. Fischer, D. M. Pyle, T. F. Yang, and G. F. Zellmer, "Fumarole compositions and mercury emissions from the Tatun Volcanic field, Taiwan: results from multi-component gas analyser, portable mercury spectrometer and direct sampling techniques," *Journal of Volcanology and Geothermal Research*, vol. 178, no. 4, pp. 636–643, 2008.

[72] A. Aiuppa, E. Bagnato, M. L. I. Witt et al., "Real-time simultaneous detection of volcanic Hg and SO_2 at La Fossa Crater, Vulcano (Aeolian Islands, Sicily)," *Geophysical Research Letters*, vol. 34, no. 21, article L21307, 2007.

[73] E. Bagnato, P. Allard, F. Parello, A. Aiuppa, S. Calabrese, and G. Hammouya, "Mercury gas emissions from La Soufrière Volcano, Guadeloupe Island (Lesser Antilles)," *Chemical Geology*, vol. 266, no. 3-4, pp. 267–273, 2009.